Article

Cell Reports

Perivascular Fibroblasts of the Developing Spleen Act as LTα1β2-Dependent Precursors of Both T and B Zone Organizer Cells

Graphical Abstract

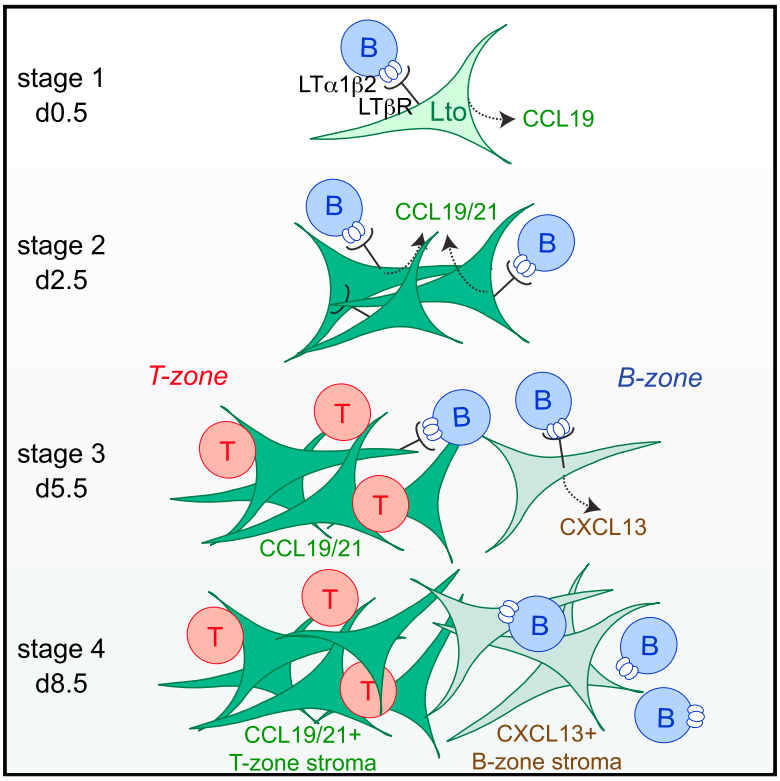

Highlights

- Postnatal splenic white pulp development proceeds in four distinct steps
- LTα1β2^{+} B cells act as inducer cells with no essential role for ILC3
- LTβR^{+}CCL19cre^{+} fibroblasts differentiate into B and T zone organizer cells
- Stromal CCL19 expression plays an important role for splenic T zone development

Authors

Karin Schaeuble, Mirjam R. Britschgi, Leo Scarpellino, ..., Alexei V. Tumanov, Jason G. Cyster, Sanjiv A. Luther

Correspondence

sanjiv.luther@unil.ch

In Brief

Schaeuble et al. describe the postnatal development and compartmentalization of splenic white pulp cords in mice, with an emphasis on stromal organizer cells. These cells are identified as fibroblasts that, upon interaction with LTα1β2^{+} B cells, differentiate into two subsets that cluster T and B cells into separate compartments.

Schaeuble et al., 2017, Cell Reports *21*, 2500–2514
November 28, 2017
https://doi.org/10.1016/j.celrep.2017.10.119

CellPress

OPEN ACCESS
CellPress

Cell Reports
Article

Perivascular Fibroblasts of the Developing Spleen Act as LTα1β2-Dependent Precursors of Both T and B Zone Organizer Cells

Karin Schaeuble,[1,6] Mirjam R. Britschgi,[1,6] Leo Scarpellino,[1] Stéphanie Favre,[1] Ying Xu,[2] Ekaterina Koroleva,[5] Tonje K.A. Lissandrin,[1] Alexander Link,[1] Mehrdad Matloubian,[2] Carl F. Ware,[3] Sergei A. Nedospasov,[4] Alexei V. Tumanov,[5] Jason G. Cyster,[2] and Sanjiv A. Luther[1,7,*]

[1]Department of Biochemistry, University of Lausanne, 1066 Epalinges, Switzerland
[2]Howard Hughes Medical Institute and Department of Microbiology and Immunology, University of California San Francisco, San Francisco, CA 94143, USA
[3]Sanford Burnham Prebys Medical Discovery Institute, La Jolla, CA 92037, USA
[4]Engelhardt Institute of Molecular Biology, Russian Academy of Sciences, 32 Vavilov Street, Moscow 119991, Russia
[5]University of Texas Health Science Center at San Antonio, San Antonio, TX 78229, USA
[6]These authors contributed equally
[7]Lead Contact
*Correspondence: sanjiv.luther@unil.ch
https://doi.org/10.1016/j.celrep.2017.10.119

SUMMARY

T and B cell compartmentalization is a hallmark of secondary lymphoid organs and is maintained by chemokine-expressing stromal cells. How this stromal cell network initially develops and differentiates into two distinct subsets is poorly known, especially for the splenic white pulp (WP). Here, we show that perivascular fibroblast precursors are triggered by LTα1β2 signals to expand, express CCL19/21, and then differentiate into two functionally distinct fibroblast subsets responsible for B and T cell clustering and WP compartmentalization. Failure to express or sense CCL19 leads to impaired T zone development, while lack of B cells or LTα1β2 leads to an earlier and stronger impairment in WP development. We therefore propose that WP development proceeds in multiple steps, with LTα1β2$^+$ B cells acting as major inducer cells driving the expansion and gradual differentiation of perivascular fibroblasts into T and B zone organizer cells.

INTRODUCTION

Secondary lymphoid organs (SLOs) are critical for mounting efficient adaptive immune responses. The spleen is the largest and primordial lymphoid organ, which has coevolved with major histocompatibility complex (MHC)-based immunity. It acts as filter for the blood and has two distinct compartments: (1) the red pulp, comprising myeloid cells and erythrocytes, along with vascular structures allowing lymphocyte entry and exit, and (2) the white pulp (WP), representing the actual lymphoid tissue with B cell-rich follicles and a T cell-rich periarteriolar lymphoid sheath (PALS) (Cyster, 2005; Neely and Flajnik, 2016). This lymphoid compartment resembles lymph nodes (LNs) and Peyer's patches (PPs) because of the typical T and B zones along with the underlying stromal fibroblast networks responsible for this segregation. Fibroblastic reticular cells (FRCs) of the T zone express CC chemokine ligand 19 (CCL19) and CCL21, which preferentially attract C-C chemokine receptor (CCR) 7$^+$ T cells and dendritic cells, while stromal cells in the B cell follicle, including follicular dendritic cells (FDCs) and marginal reticular cells (MRCs), express CXC chemokine ligand (CXCL) 13 and attract CXC chemokine receptor (CXCR) 5$^+$ B cells (Cyster, 2005; Randall et al., 2008; Roozendaal and Mebius, 2011), thereby establishing the two major compartments.

Combined deficiency in these three chemokines or their receptors leads to the absence of most LNs and PPs and to very small and disorganized WP cords, pointing to a critical role of chemokine-expressing cells, presumably fibroblasts, in organ development and structure (Luther et al., 2003; Ohl et al., 2003). Consistent with this notion, ectopic expression of CCL21 or CXCL13 is sufficient to induce lymphoid tissue-like structures (Luther et al., 2002).

The process of SLO organogenesis has been defined in detail for murine LN anlagen, which start developing during embryogenesis (Randall et al., 2008; Roozendaal and Mebius, 2011). Key to this process are not T and B lymphocytes but LTα1β2$^+$CD4$^+$CD3$^-$ lymphoid tissue inducer (LTi) cells, now known as type 3 innate lymphoid cells (ILC3), which engage in a crosstalk with stromal organizer cells (LTo) expressing the LTβ receptor (LTβR). Very recent work suggests that LTβR, receptor activator of nuclear factor κB (RANK), and the common downstream signaling molecule nuclear factor κB-inducing kinase (NIK) need to be triggered initially in lymphatic endothelial cells for LN anlagen to develop and only later on in blood endothelial and fibroblastic stromal cells for further organ development and patterning (Chai et al., 2013; Onder et al., 2017). LTα1β2 signals are critical to induce the expression of CCL19, CCL21, and CXCL13 by fibroblastic LTo cells, in addition to other cytokines and adhesion molecules, thereby leading to the clustering and accumulation of more ILC3 cells and eventually lymphocytes that express the corresponding chemokine receptors CCR7 and CXCR5 (Chai et al., 2013; Randall et al.,

2008; Roozendaal and Mebius, 2011). Accordingly, *Lta*-, *Ltb*-, or *LTbr*-deficient mice as well as mice lacking ILC3 because of absence of the transcriptional regulator RAR-related orphan receptor (ROR) γ or Id2 have severe impairment in LN and PP development.

The processes and cellular interactions leading to splenic WP development are only partially understood (Neely and Flajnik, 2016; Randall et al., 2008; Roozendaal and Mebius, 2011). In mice, the spleen is first detectable around E10, consisting essentially of red pulp, but the WP structure resembling a lymphoid organ becomes visible only around birth, when lymphocytes start entering the organ and increasingly accumulate in clusters around central arterioles (Friedberg and Weissman, 1974; Katakai et al., 2008; Vondenhoff et al., 2008). Importantly, absence of B cells but not ILC3 or T cells is associated with prominent defects in WP organization of adult mice, including strongly reduced levels of *Cxcl13* and *Ccl21*, as well as small and disorganized WP cords (Ngo et al., 2001; Zhang et al., 2003). Similar WP defects are observed in adult mice lacking LTα, LTβ, or LTβR, suggesting that all major SLOs develop in a conserved process, with LTα1β2 signals being provided by hematopoietic inducer cells to LTβR-expressing LTo cells, leading to chemokine expression that is responsible for lymphocyte attraction, retention, and finally segregation (Randall et al., 2008; Tumanov et al., 2003).

Although splenic FDCs continuously depend on LTα1β2 and TNF-α signals provided by B cells (Cyster, 2005; Tumanov et al., 2003), the situation is less clear for the development of splenic T zone FRCs. Injection of LTβR-Fc into d0.5 pups but not d7 pups led to a major defect in CCL21^{+} podoplanin^{+} FRCs in the adult spleen (Ngo et al., 2001), reminiscent of B cell-deficient spleens. As day 4 splenic B cells express surface LTα1β2, these cells were proposed to be the inducer cells of splenic WP development during the first week of life, consistent with LTαβ-transgenic B cells being sufficient to rescue WP development in *Lta*$^{-/-}$ mice (Ngo et al., 2001; Vondenhoff et al., 2008). However, analysis of adult spleens from mice with B cell-specific *Ltb* deletion did not fully support this notion (Tumanov et al., 2002, 2003). In addition, spleens of *Rag*$^{-/-}$ mice reconstituted with *Lta*-deficient lymphocytes developed well segregated B and T cell-rich zones, including CCL21^{+} podoplanin^{+} FRC networks, suggesting that ILC3 may contribute as a LTα1β2^{+} source to the postnatal development of chemokine-expressing stromal cells (Kim et al., 2007; Withers et al., 2007). This model is supported by the observation of ILC3 in the periarteriolar region of embryonic and perinatal spleen (Vondenhoff et al., 2008; Withers et al., 2007) but inconsistent with the grossly normal WP structure in spleens of adult RORγ$^{-/-}$ mice (Zhang et al., 2003). Together, these contradictory data highlight the need for a reevaluation of the critical LTα1β2 source in this process, including a more detailed analysis of neonatal rather than adult spleen cells and tissues.

In contrast to embryonic LN and PP anlagen, the stromal organizer cells of the neonatal WP have been poorly characterized in mice, in part because of the lacking expression of typical FDC and FRC markers, such as CD35, podoplanin (gp38), and BP-3 on neonatal WP (Balogh et al., 2001; Bekiaris et al., 2007; Qin et al., 2007). Vascular cell adhesion molecule-1 (VCAM-1)$^{+}$ stromal cells clustering with ILC3 were observed starting around E16.5 (Vondenhoff et al., 2008; Withers et al., 2007), but the function of this interaction has remained unclear. Recently, fate mapping using mesenchymal-specific reporter lines on the basis of the transcription factors Nkx2–5 and Islet-1 have suggested that all splenic fibroblast subsets derive from a common embryonic precursor (Castagnaro et al., 2013). At E18.5, these cells showed features reminiscent of LTo activity, including *Ltbr* and *Cxcl13* expression. However, we lack a good understanding of the splenic LTo involved in the early postnatal phase when the lymphoid aspect of the spleen develops.

The aims of this study were to obtain a detailed understanding of postnatal splenic WP organogenesis and compartmentalization, to identify and track the chemokine-expressing LTo cell types through development and specialization, and to shed more light on the LTα1β2-expressing lymphoid tissue inducer cells responsible for LTo activation and differentiation. Evidence is provided for several distinct LTα1β2-induced stages of LTo cell and WP development that allow to propose a much more refined model of how the body's largest lymphoid organ develops.

RESULTS

CCR7, but Not CXCR5, Is Important for Early Steps in WP Development

Histological analysis of lymphocytes in murine spleen sections at various time points after birth shows four distinct developmental stages, as based on the spatial organization of T and B lymphocytes (Figure 1A). On postnatal day (d) 0.5, only a few B cells are found scattered around central arterioles (stage 1), while on d2.5, an increasing number of B cells cluster around these vessels in the presence of very few T cells (stage 2). On d5.5, T cells have accumulated close to the central arteriole, and the B cells are displaced outward into a ring-like structure but not yet forming clearly segregated zones (stage 3). The fourth stage starts around d8.5, when a larger T cell area has developed in the central WP, with B cells being clustered in clearly segregated and increasingly polarized follicles that form the outer WP region. After d8.5, the WP area continues to grow until it reaches close to adult size at 3–4 weeks of age (Figure 1A).

As adult mice with combined deficiency in CXCR5 and CCR7 lack organized splenic WP areas (Ohl et al., 2003), the role of these two receptors in neonatal WP development was investigated. T lymphocytes isolated from d5.5 spleen expressed CCR7, while B cells expressed both CCR7 and CXCR5 (Figure 1B). The functionality of these chemokine receptors was confirmed in migration assays, with lymphocytes from d5 spleen migrating efficiently toward CCL19, CCL21, and CXCL13 (Figure 1C).

To investigate whether neonatal lymphocytes depend on CCR7 and/or CXCR5 for entry and positioning within the neonatal spleen, T and B cell distribution was assessed in d5.5 spleens of *Ccr7*$^{-/-}$ and *Cxcr5*$^{-/-}$ mice. In the absence of CCR7, T cells were rare, with the WP consisting mainly of B cells localized around the central arteriole (Figure 1D), consistent with reduced absolute T cell numbers (Figure 1E), as reported previously (Ueno et al., 2002, 2004). At 3.5 weeks of age, T and B

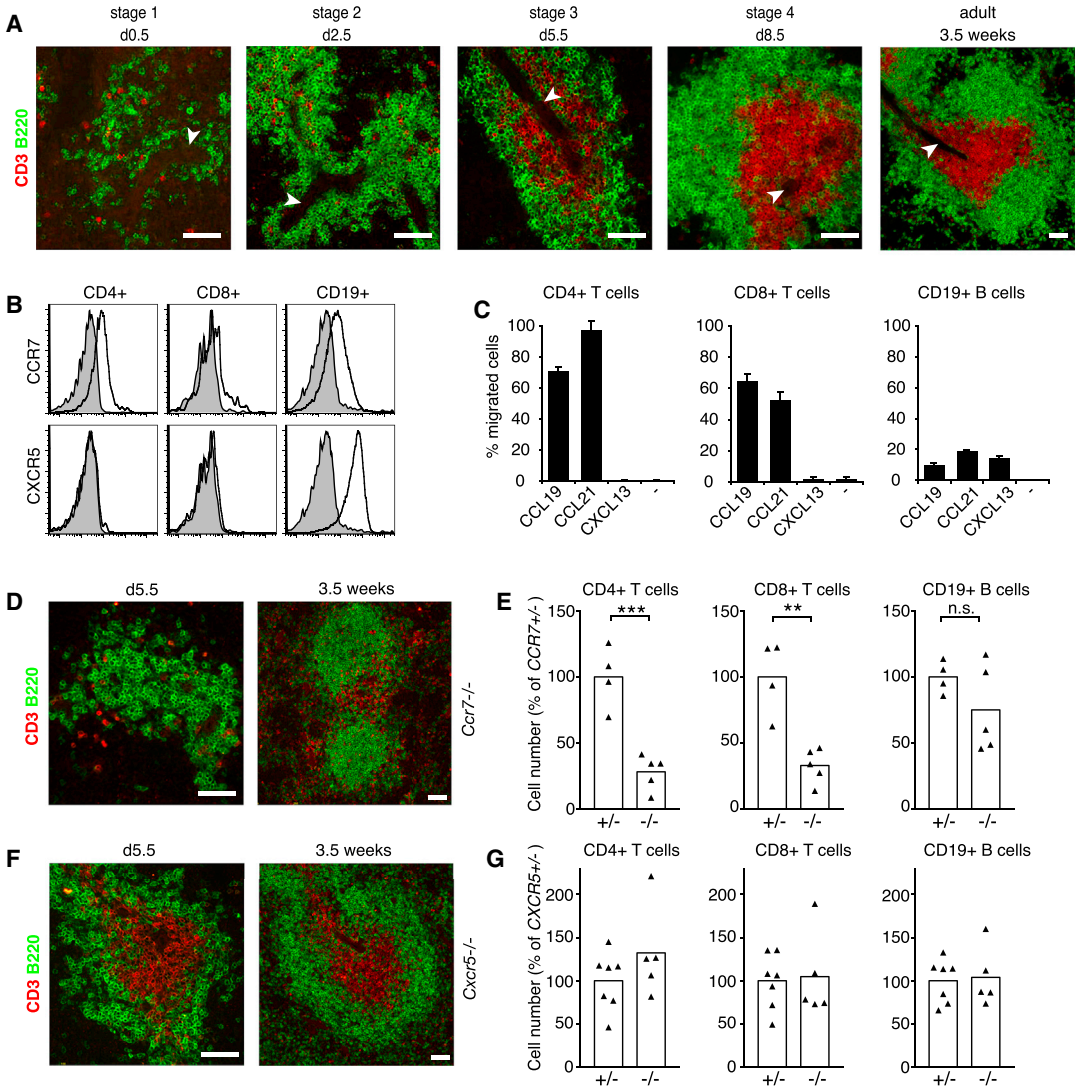

Figure 1. CCR7, but Not CXCR5, Is Critical for White Pulp Colonization by T Lymphocytes

(A) Immunofluorescence staining on wild-type (WT) murine spleen sections at different stages of development (d, days after birth) for $CD3^+$ T cells and $B220^+$ B cells. Arrowheads indicate the central arteriole (CA). n = 4 per time point.

(B) Flow cytometric analysis of CCR7 and CXCR5 chemokine receptor expression on $CD4^+$ and $CD8^+$ T lymphocytes and $CD19^+$ B lymphocytes from d5.5 spleen of WT mice (in gray shading, isotype-matched control antibody), representative of five independent experiments.

(C) Three hour transwell chemotaxis assay of splenocytes from d5.5 WT neonates toward 0.2 μg/mL CCL19, 1 μg/mL CCL21, 1 μg/mL CXCL13, or medium alone (–), representing one of two independent experiments.

(D) Immunofluorescence staining for T and B cells on spleen sections of $Ccr7^{-/-}$ mice at d5.5 and 3.5 weeks.

(E) Cell numbers of $CD4^+$ and $CD8^+$ T cells as well as $CD19^+$ B cells in the spleen of d6.5 $Ccr7^{-/-}$ (n = 5) compared with $Ccr7^{+/-}$ (n = 4) neonates. Similar results were obtained with *plt*/*plt* animals.

(F) Immunofluorescence staining for T and B cells on spleen sections of $Cxcr5^{-/-}$ mice at d5.5 and 3.5 weeks.

(G) Lymphocyte numbers in spleen of d5.5 $Cxcr5^{-/-}$ (n = 5) neonates compared with $Cxcr5^{+/-}$ (n = 7) littermates. Data are representative of three independent experiments.

Histological data shown in (D) and (F) are representative of several WP areas in two or three mice per group. Scale bars represent 50 μm.

zones had formed in $Ccr7^{-/-}$ spleens, but the T zone size remained small, with many T cells found in the RP (Figure 1D) (Förster et al., 1999). In the absence of CXCR5, T and B zones appeared normal in d5.5 spleens, suggesting that the initial WP development occurs in a CXCR5-independent manner (Figure 1F). Consistent with this observation, splenic B and T cell numbers were not altered in d5.5 $Cxcr5^{-/-}$ versus $Cxcr5^{+/-}$ mice (Figure 1G). As expected (Ansel et al., 2000; Förster et al., 1996), B cell follicles failed to polarize in spleens of 3.5-week-old $Cxcr5^{-/-}$ mice (Figure 1F). In conclusion, CCR7 but not CXCR5 has an essential organizer role during early WP development.

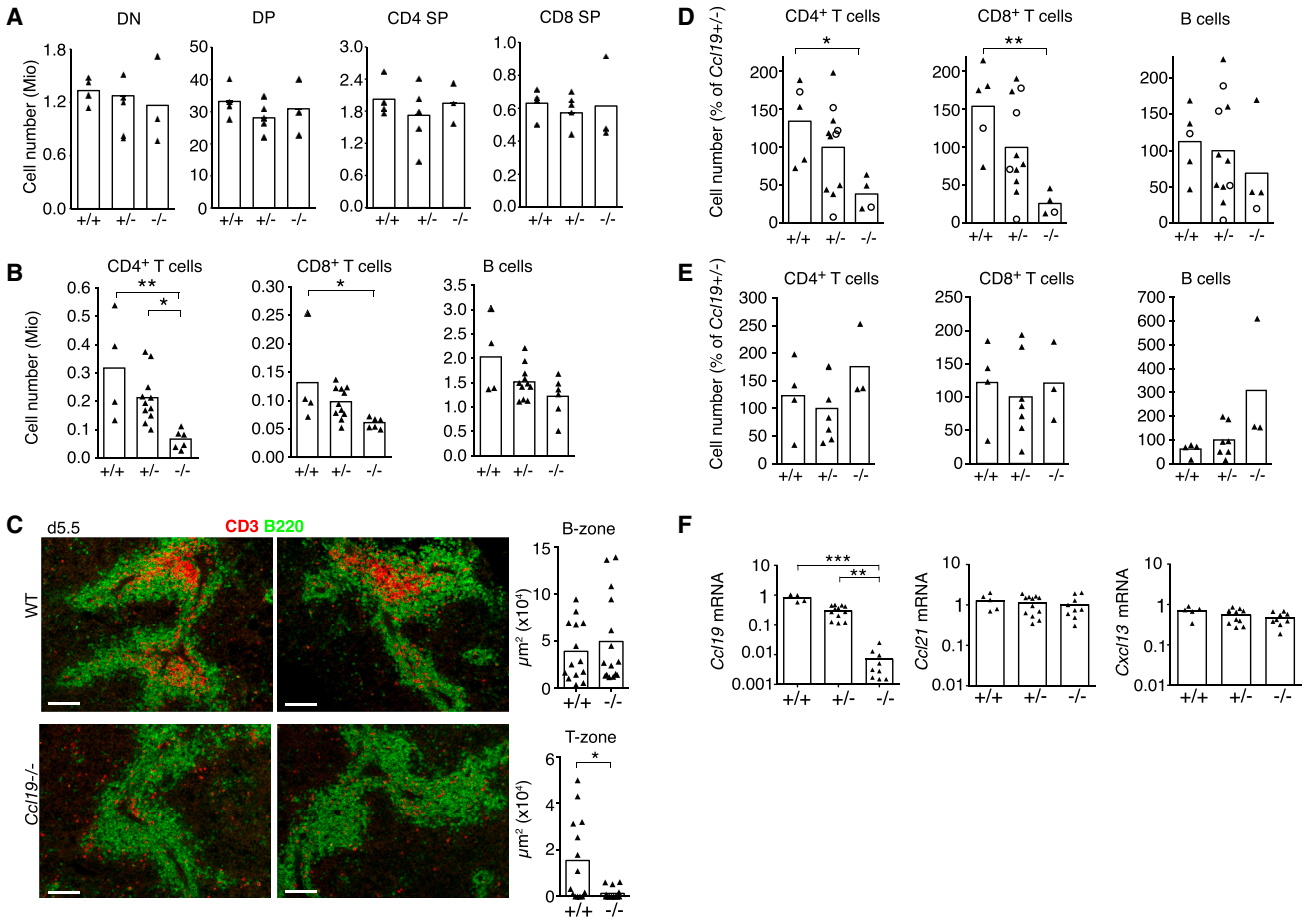

Figure 2. *CCL19* Is Important for T Cell Homing into the Neonatal Spleen but Not LNs

(A) Flow cytometric analysis of thymocyte populations of d5.5 *Ccl19*$^{+/+}$, *Ccl19*$^{+/-}$, and *Ccl19*$^{-/-}$ littermates: double negative (DN) (CD4$^-$ CD8$^-$), double positive (DP) (CD4$^+$ CD8$^+$), CD4 single positive (SP) (CD4$^+$ CD8$^-$), and CD8 SP (CD4$^-$ CD8$^+$). Data are representative of two independent experiments. Similar results were obtained with d3.5 animals.

(B) Lymphocyte numbers in spleens of d5.5 *Ccl19*$^{+/+}$ (n = 4), *Ccl19*$^{+/-}$ (n = 11), and *Ccl19*$^{-/-}$ (n = 6) littermates. Similar results were obtained with pups aged 3 and 6 days.

(C) Immunofluorescence staining for T and B cells on spleen sections from d5.5 WT (*Ccl19*$^{+/+}$) versus *Ccl19*$^{-/-}$ littermate mice. Two representative examples are shown. Quantification of B220$^+$ B and CD3$^+$ T cell areas in several splenic WP sections of d5.5 *Ccl19*$^{-/-}$ and WT littermates. n $\geq$ 2 per genotype. Scale bars represent 100 µm.

(D and E) Flow cytometric analysis of CD45.1$^+$ lymphocytes in spleen (D) and peripheral LNs (E) 5 days after adoptive transfer into d1.5 (triangles) or d0.5 (open circles) *Ccl19*$^{+/+}$, *Ccl19*$^{+/-}$, and *Ccl19*$^{-/-}$ littermates (all CD45.2$^+$); data were compiled from three (D) or two (E) independent experiments. Triangles and open circles represent data from individual mice, and bars represent the means.

(F) Relative mRNA expression levels of *Ccl19*, *Ccl21*, and *Cxcl13* as assessed by real-time RT-PCR from spleens of d5.5 *Ccl19*$^{+/+}$ (n = 5), $^{+/-}$ (n = 12), and $^{-/-}$ (n = 9) littermate mice, respectively.

CCL19 Is Critical for Proper Formation of Splenic T Zones

It was proposed that the reduced splenic T cell numbers in neonatal *Ccr7*$^{-/-}$ mice are secondary to a thymic exit defect and caused mostly by the absence of CCL19 signaling (Ueno et al., 2002), but later data from the same group showed relatively normal thymocyte numbers in *Ccr7*$^{-/-}$ and *plt/plt* (*Ccl19/21*$^{-/-}$) neonates (Ueno et al., 2004), consistent with our own findings for these two strains (not shown). To gain further insight, we analyzed neonatal *Ccl19*$^{-/-}$ mice. No significant difference was observed in the size of the various thymocyte subsets in d5.5 *Ccl19*$^{-/-}$ mice compared with littermates (Figure 2A). Nevertheless, CD4$^+$ and CD8$^+$ T but not B cell numbers were strongly reduced in the spleen of d5.5 *Ccl19*$^{-/-}$ mice (Figure 2B), leading to markedly smaller T zone areas (Figure 2C). In contrast, lymphocyte numbers in LNs were normal (not shown). The splenic T cell accumulation defect proved to be thymus independent and T cell extrinsic as adoptive transfers of adult wild-type (WT) lymphocytes into d0.5–1.5 *Ccl19*$^{-/-}$ neonates reproduced the adult *Ccl19*$^{-/-}$ spleen phenotype while showing normal homing to LNs (Figures 2D and 2E). Analysis of d5.5 spleen transcript levels confirmed that *Ccl19*$^{-/-}$ mice lack only *Ccl19* expression, with no alterations of *Ccl21* and *Cxcl13* (Figure 2F). Together, our results show that CCL19 deficiency causes

defective T cell accumulation in the nascent WP with the second CCR7 ligand, CCL21, not being able to compensate for this defect.

LTα1β2-Dependent Expression of Homeostatic Chemokines Occurs in Distinct Waves

To better understand the role of chemokines in WP formation we assessed the expression pattern of *Ccl19*, *Ccl21*, and *Cxcl13* transcripts. *Ccl19* mRNA expression was strongly induced around birth and reached the 50-fold higher adult levels by d8.5 (Figure 3A). In contrast, *Ccl21* transcripts were already highly expressed on d0.5 and dropped almost 10-fold on d2.5, and this was followed by a steady increase into adulthood. Finally, *Cxcl13* transcripts were high from d0.5 onward and showed only a small change over time. These results indicate that the expression and regulation of these three chemokines is surprisingly diverse.

Transcripts of these three chemokines have been reported to be present both in mesenchymal and vascular cells of embryonic spleen (Castagnaro et al., 2013; Vondenhoff et al., 2008) and proposed to be LTαβ independent, as hardly any LTα1β2-expressing cells were found at birth (Vondenhoff et al., 2008). To identify the time point of LTα1β2-dependent chemokine induction, the levels of the three chemokines were assessed at various times in neonatal spleen of $Lt\alpha^{-/-}$ versus WT mice. Whereas *Ccl19* expression was LTα1β2 dependent at all time points, including d0.5, *Ccl21* expression became LTα dependent only by d5.5 and *Cxcl13* by d8.5 (Figure 3A). The LTα-dependent induction of *Ccl19* at a time when no T cells were present in the spleen suggested that B cells or ILC3 were the likely LTα1β2 source. To investigate the B cell requirement for chemokine expression, transcripts from neonatal spleens of B cell-deficient mice ($Bcr^{-/-}$) were analyzed (Figure 3A). Strikingly, at all time points investigated *Ccl19* transcripts were reduced to the same extent as in $Lta^{-/-}$ spleen. *Ccl21* and *Cxcl13* expression was similarly dependent on B cells as on LTα, starting on days 5.5 and 8.5, respectively. Taken together, these genetic data suggest that B cells are the critical LTα source during WP development.

IgD$^+$ IgM^{high} B Cells Are the Major LTα1β2 Source in Neonatal Spleen Development

The relative contribution of B cells and ILC3 as LTα1β2 source in postnatal WP development is controversial (Ngo et al., 2001; Tumanov et al., 2003; Vondenhoff et al., 2008; Withers et al., 2007). As we observed LTα1β2-dependent *Ccl19* expression on d0.5 when no LTα1β2-expressing cells have been detected in a previous study (Vondenhoff et al., 2008), we reinvestigated this issue by measuring surface LTα1β2 levels on postnatal splenocytes. At all time points investigated, LTα1β2 expression was observed mainly on B cells and ILC3 and at later stages also on T cells (Figures 3B, 3C, S1A, and S1B). B cells express very low levels of surface LTα1β2 at birth, but this level increases gradually thereafter (Figures 3B and 3C) (Vondenhoff et al., 2008). Among the B cell subsets investigated, the highest LTα1β2 expression was found on IgD$^+$ IgM^{high} cells representing mature B cells (Figures 3B and S1A). In addition, we observed 40%–50% of ILC3 expressing high LTα1β2 levels, independently of the time point investigated (Figures 3C and S1B). However, LTα1β2$^+$ ILC3 are relatively rare cells with LTα1β2$^+$ B cells outnumbering them at all time points investigated, with B cells being 7, 16, and 180 times more frequent on d0.5, d2.5, and d5.5, respectively (Figure 3C). Consistent with this finding, *Lta* and *Ltb* transcripts were enriched in IgM^{high} B cells of d5.5 neonatal spleen, with intermediate levels in IgM^{low} B cells and low levels in the less frequent CD19$^-$CD4$^-$CD45$^+$ splenocytes (Figure 3D). To test genetically a role for LTα1β2$^+$ B cells in WP development, d8.5 spleens of mice with a B cell-specific *Ltb* deletion (*Cd19-cre* × $Ltb^{fl/fl}$) were investigated. Seventy-five percent of the floxed *Ltb* loci were deleted in sorted B cells (Figure S1C). As a consequence, transcripts of all three chemokines were reduced by 50%–70%, although *Ccl19* and *Ccl21* levels stayed somewhat above those in $Ltb^{-/-}$ and $Lta^{-/-}$ spleens (Figure 3E), possibly because of the incomplete *Ltb* deletion in B cells. In summary, our evidence points to B cells being an important LTα1β2 source within the postnatal WP cords.

LTβR$^+$ Desmin$^+$ Fibroblasts Act as Chemokine-Expressing Organizer Cells

To determine the chemokine-expressing cell types, we fractionated the neonatal spleen into hematopoietic versus stromal cells. Transcripts for all three chemokines were enriched 10- to 5,000-fold in the stromal cell fraction (Figure 4A), similar to adult spleen (Link et al., 2007). Next, neonatal spleen suspensions were analyzed by flow cytometry for LTβR$^+$ stromal cells. Among CD45$^-$ cells, only around 3.5% of d10 splenocytes expressed surface LTβR (Figure 4B), mostly because of the presence of many Ter119$^+$ erythroblasts. Similar to adult spleen (Fasnacht et al., 2014), LTβR$^+$ cells could be subdivided into CD31$^-$ non-vascular cells and CD31$^+$ vascular cells (Figure 4B). Similar data were obtained for d5.5 and d2.5 spleens (Figures S2A and S2B), but given the higher cell numbers in d10 spleen, this time point was chosen to sort various cell populations suspected to be chemokine sources. LTβR$^+$ CD31$^-$ cells were the most abundant source of *Ccl19*, *Ccl21*, and *Cxcl13* mRNA with at least 30-fold higher expression than in LTβR$^+$ endothelial cells, other CD45$^-$ cells, or pooled CD45$^+$ cells (Figure 4C). Further phenotypic analysis of both LTβR$^+$ stromal cell fractions revealed that the CD31$^-$ stromal cells in d5.5–d6.5 spleen expressed platelet-derived growth factor receptor (PDGFR) α, PDGFRβ, VCAM-1, intercellular adhesion molecule-1 (ICAM-1), endoglin, CD44, and intracellular desmin (Figure 4D; Table S1), similar to d2.5 spleens (Figure S2C). Only a very small subset of CD31$^-$ stromal cells express podoplanin, while no BP-3 was detectable at that stage (Figure 4D), suggesting that these cells were of mesenchymal nature but not yet fully matured relative to their adult counterparts (Link et al., 2007).

Some of the identified stromal markers were then used to define the localization and organization of these stromal cells (Figure 4E). Histological analysis confirmed that reticular podoplanin and BP3 staining was observed only from day 8 onward (Figure S3A) (Balogh et al., 2001; Bekiaris et al., 2007; Qin et al., 2007). However, podoplanin was frequently expressed by vessels displaying many characteristics of lymphatics (Lyve1$^+$CD31$^+$ Prox1$^+$ VEGFR3$^+$ Meca32$^-$), including LTβ-independent CCL21 protein expression. These vessels were frequent

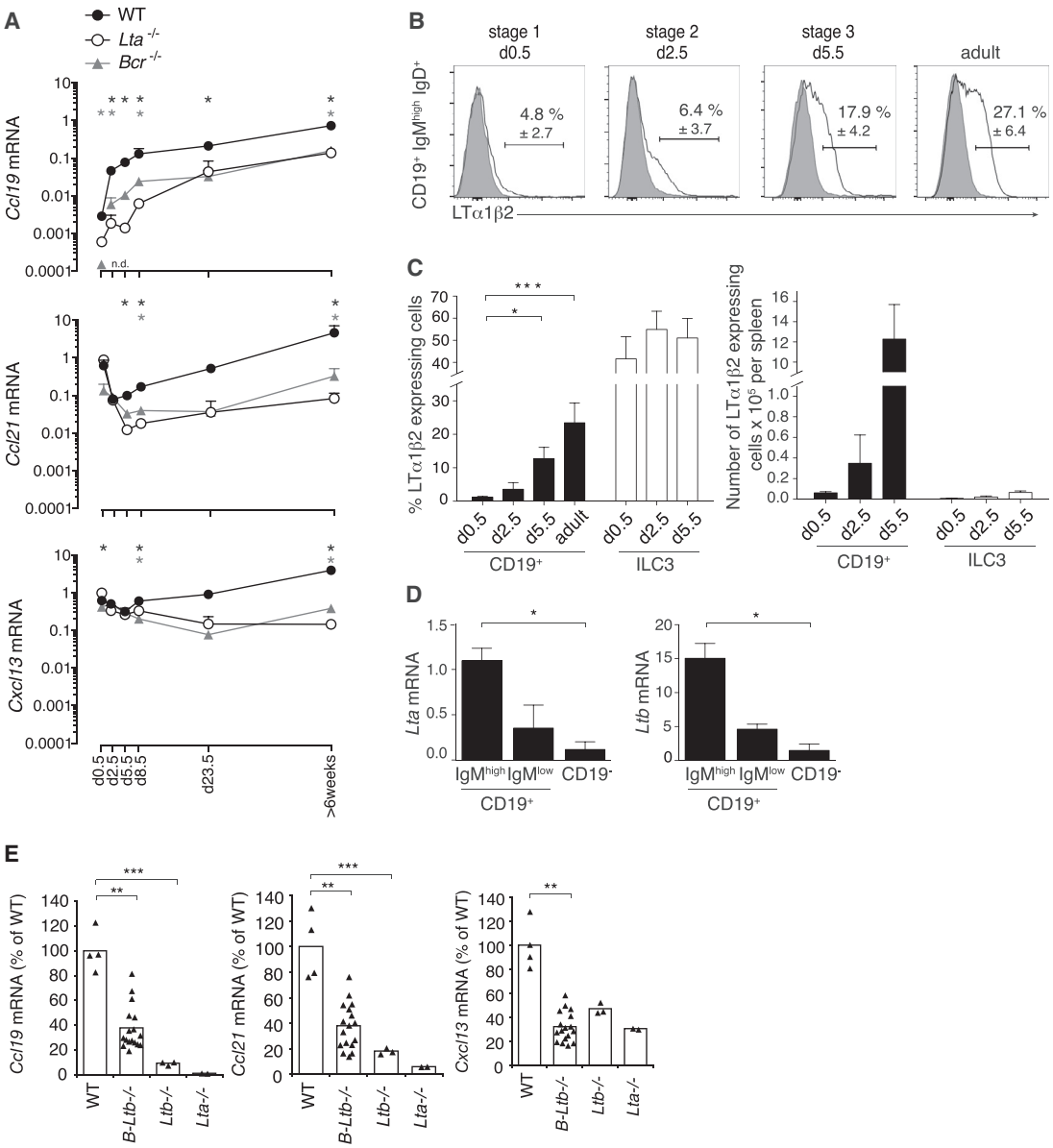

Figure 3. Chemokine Expression in the Developing WP Shows a Sequential Dependence on Lymphotoxin that Is Provided Mainly by Mature B Cells during Postnatal WP Development

Real-time PCR analysis for the expression of *Ccl19*, *Ccl21*, and *Cxcl13* in total spleen at different time points after birth.

(A) Relative transcript levels in spleens of WT versus *Lta*$^{-/-}$ and *Bcr*$^{-/-}$ mice. Data are representative of n = 3 mice/genotype for all time points except day 23.5 and the day 0.5 *Lta*$^{-/-}$ sample (n = 2).

(B) Flow cytometry analysis of surface LTα1β2 expression on splenic CD19^{+} IgM^{high} IgD^{+} B cells of WT neonates at the indicated days after birth, using LTβR-Fc (white shading) versus LTβR-Fc preblocked with a LTβ-neutralizing antibody (gray shading) to highlight the LTα1β2-specific signal.

(C) Frequency and number of LTα1β2-expressing CD19^{+} B cells and CD45^{+} CD4^{+} CD3^{-} or TCRβ^{-} CD19^{-} cells (ILC3) in the spleen of neonatal and adult WT mice. Data in (B) and (C) are representative of n ≥ 4 samples per time point.

(D) Real-time PCR to assess *Lta* and *Ltb* transcript levels in sorted B cells (IgM^{high} versus IgM^{low} CD19^{+}CD45^{+}) and CD19^{-} CD4^{-} cells from a pool of d2.5 WT spleens.

(E) Real-time PCR to assess chemokine expression in spleens of d8 *Ltb*$^{fl/fl}$ (WT, n = 4), *Cd19-Cre*$^{+}$ *Ltb*$^{fl/fl}$ (*B-Ltb*$^{-/-}$, n = 17), *Ltb*$^{-/-}$ (n = 3), and *Lta*$^{-/-}$ (n = 2) mice displayed as percent of average WT level.

See also Figure S1.

in d0–d5 spleen and often found at the edge of developing WP cords but rare and ensheathed in trabeculae of adult spleen (Figures S3B–S3F), confirming past reports on adult spleen (reviewed in Shimizu et al., 2009).

Known markers for LN mesenchyme identification, such as ICAM-1, VCAM-1, and mucosal vascular addressin cell adhesion molecule-1 (MAdCAM-1), were not very specific for splenic mesenchymal cells. VCAM-1 expression was found all over the

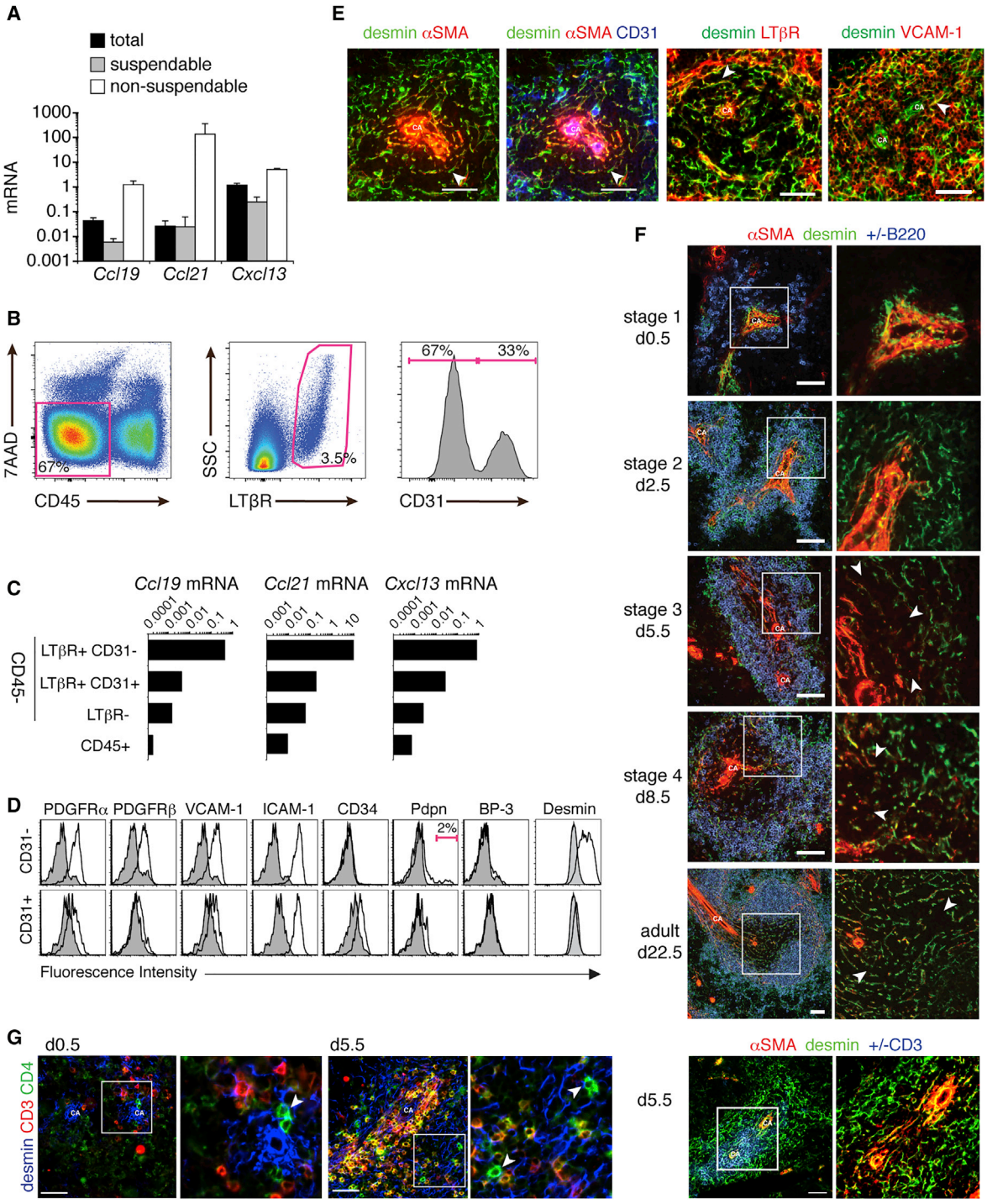

Figure 4. LTβR-Expressing Mesenchymal Cells Are the Major Chemokine Source in Nascent WP Cords

(A) Real-time PCR analysis for the expression of *Ccl19*, *Ccl21*, and *Cxcl13* on either unfractionated spleen (total) or from suspendable (hematopoietic) or non-suspendable (stromal) spleen fractions from d5.5 WT mice (n = 3). Similar results were obtained for d2.5 spleen fractions.

(B–D) Single-cell suspensions from d10.5 (B and C) and d6.5 (D) spleens digested by collagenase and stained with surface markers while excluding dead cells ($7AAD^+$). (B) Flow cytometric gating strategy to identify two subsets of $LT\beta R^+$ $CD45^-$ stromal cells: $CD31^-$ reticular cells and $CD31^+$ vascular cells. (C) RT-qPCR for *Ccl19*, *Ccl21*, and *Cxcl13* mRNA levels in the indicated three $CD45^-$ and one $CD45^+$ splenocyte population. (D) Flow cytometry histograms showing the expression of additional markers (black line) on the surface of $CD31^-$ reticular and $CD31^+$ vascular cells (gray shading, no primary antibody control). $n \geq 2$.

(E–G) Immunofluorescence staining of splenic sections with the markers and at the days after birth indicated. (E) d5.5 spleen with arrowheads pointing out $desmin^+$ mesenchymal cells localized within the nascent WP and their expression of other stromal cell markers (αSMA, LTβR, VCAM-1, but not CD31 that marks

(legend continued on next page)

d5 spleen, on both reticular cells and vessels; ICAM-1 stained most WP cells, including lymphocytes, and MAdCAM-1 was found only in the outer WP, including on vessels (Figures 4D and 4E; data not shown) (Vondenhoff et al., 2008). Among the other mesenchymal markers, desmin staining appeared to highlight best the sites of nascent WP cords where B220$^+$ B cells clustered and laminin$^+$ fibers were apparent (Figures 4E, 4F, S3A, S4A, and S4B). In day 5 spleen, desmin$^+$ cells formed a reticular network around the α-smooth muscle actin (αSMA)$^+$ central arteriole and covering the whole B cell area, with a denser reticular network encircling the B cell clusters (Figures 4F and S4A). Desmin$^+$ cells expressed LTβR in addition to VCAM-1 and PDGFRβ (Figures 4D and 4E). The presence of various mesenchymal markers along with their fibroblastic morphology and association with laminin fibers indicated that these LTβR$^+$ cells are fibroblasts.

In d5.5 spleen, αSMA expression labeled only desmin$^+$ fibroblasts of the inner WP, in addition to its strong expression on desmin$^+$ smooth muscle cells wrapping around the CD31$^+$ central arteriole (Figures 4E and 4F). Therefore, WP cords were investigated at different time points using αSMA and desmin as markers (Figures 4F and S4B). On d0.5, few desmin$^+$ reticular cells were observed adjacent to αSMA$^+$ smooth muscle cells enwrapping the central arteriole, with the first scattered B cells being grouped around it. On d2.5, a small αSMA$^-$ desmin$^+$ reticular cell network had formed around the central arteriole and throughout the growing B cell cluster. From d5.5 onward, two types of WP reticular cells could be distinguished: an outer ring of desmin$^+$ αSMA$^-$ cells colocalizing with B cells, and an inner zone of desmin$^+$ αSMA$^+$ cells colocalizing with T cells (Figure 4F). CD4$^+$3$^-$ ILC3 localized similarly as B cells, close to the central arteriole on d0.5 and in the outer WP on d5.5, but always within the desmin$^+$ reticular network (Figure 4G). In conclusion, our data demonstrate that the organization into T and B zones in the postnatal WP is accompanied by distinct stromal fibroblast networks in each zone, distinguishable by desmin and αSMA expression.

CCL19cre-Expressing Fibroblasts Act as Precursors of Both B and T Zone Fibroblasts

To further substantiate the existence of two fibroblast subsets in d5 WP cords, we performed *in situ* hybridization for lymphoid tissue chemokines in combination with antibody staining for desmin and αSMA (Figure 5A). *Ccl19* and *Ccl21* mRNA co-localized with desmin$^+$ αSMA$^+$ fibroblasts of the inner WP, while *Cxcl13* mRNA was produced by a thin rim of desmin$^+$ αSMA$^-$ fibroblasts of the outer WP. The co-staining revealed a third outermost WP stromal cell layer expressing high levels of desmin but no detectable *Cxcl13* mRNA. As MAdCAM-1 expression is very prominent in that zone, these latter fibroblasts may participate in MZ development (Zindl et al., 2009). A similar functional segregation into T and B zone stroma was observed in d5 spleen by antibody labeling of CCL19, CCL21, and CXCL13 protein with CCL19 protein colocalizing with desmin$^+$ cells of the T cell zone and CXCL13 protein predominantly with desmin$^+$αSMA$^-$ cells of the B cell zone (Figure 5B). High CCL21 protein expression was enriched in the inner WP, but lower levels were also apparent in the outer WP. In addition, CCL21 protein was also seen on lymphatic vessels (Figures 5B and S3B).

Having previously observed high levels of *Ccl21* and *Cxcl13* transcripts in d0.5 spleen and the strong induction of *Ccl19* mRNA between d0.5 and d2.5, we wished to identify the chemokine-expressing cells at these earlier times, by both antibody staining and fate mapping using *Ccl19-cre* crossed to *Rosa26-eyfp$^{fl/fl}$* reporter mice. In d0.5 spleen, only single reticular EYFP$^+$ cells were visible next to central arterioles, consistent with very little CCL19 protein being detectable (Figure 5C). On d2.5, the EYFP$^+$ reticular network was strongly enlarged around the central arteriole, with many cells expressing CCL19 protein and correlating in time with first T cells localizing to the inner WP zone. In d5.5 spleen, the EYFP$^+$ reticular cell network comprised the zones occupied by both T and B cells. The CCL19 protein staining colocalized with reticular EYFP$^+$ cells of the inner but not outer WP, suggesting that CCL19 expression is low or has been downregulated in EYFP$^+$ cells of the outer WP or their precursors (Figure 5C). On d5.5, almost all reticular EYFP$^+$ cells expressed CCL21 protein, while CXCL13 protein colocalized only with the outer rim of EYFP$^+$ cells. These findings indicate functional specialization among WP fibroblasts, with all of them being derived from cells having expressed at one point *Ccl19* transcripts. In contrast to CCL19, expression of CCL21 and CXCL13 protein was already detected in d0.5 spleens. CCL21 protein is present at high levels on lymphatic vessels, often outside the developing WP cords, with their frequency decreasing between d0.5 and d5.5 correlating with the drop in *Ccl21* transcripts (Figures 3A, 5C, and S3B). Within the developing WP, CCL21 expression was visible on d0.5 only on central arteriole-associated perivascular cells, with reticular CCL21 staining starting from d2.5 onward on EYFP$^+$ cells. In contrast, in d0.5 spleens, CXCL13 protein labeled only central arteriole-associated perivascular cells, which were EYFP$^-$ CD34$^-$ desmin$^+$ (Figure 5C; not shown). This perivascular staining persisted up to d5.5, but in addition CXCL13 protein became visible on EYFP$^+$ reticulum of the outer WP. Together, our data demonstrate that LTβR$^+$CD31$^-$ cells identified by flow cytometry as major chemokine source can be mapped histologically to desmin$^+$ fibroblast networks that organize WP cords, with a functional specialization detectable around d5.5.

Mice Deficient in B Cells or LTβ Fail to Trigger the Growth and Differentiation of the Early B and T Zone Stromal Cell Networks

Next, we asked what cells and signals are required for development of αSMA$^+$ T zone fibroblasts expressing CCL19/21, and

the CA). Data are representative of three independent experiments (E and F). (F) αSMA and desmin staining identifying the sites of early lymphocyte clustering and showing the gradual development of the splenic WP stroma, along with its differentiation into αSMA$^+$ desmin$^+$ T zone and αSMA$^-$ desmin$^+$ B zone fibroblasts. White rectangles indicate the area of higher resolution shown on the right (F and G). Arrowheads indicate desmin$^+$ αSMA$^+$ stromal cells in the inner WP, proximal to the αSMA$^+$ smooth muscle layer around the CA. (G) ILC3 (CD3$^-$ CD4$^+$) are indicated by white arrowheads and colocalize also with desmin$^+$ WP fibroblasts. White rectangles indicate the area of higher resolution on the right. Scale bars represent 25 μm (E) and 50 μm (F and G).
See also Figures S2–S4 and Table S1.

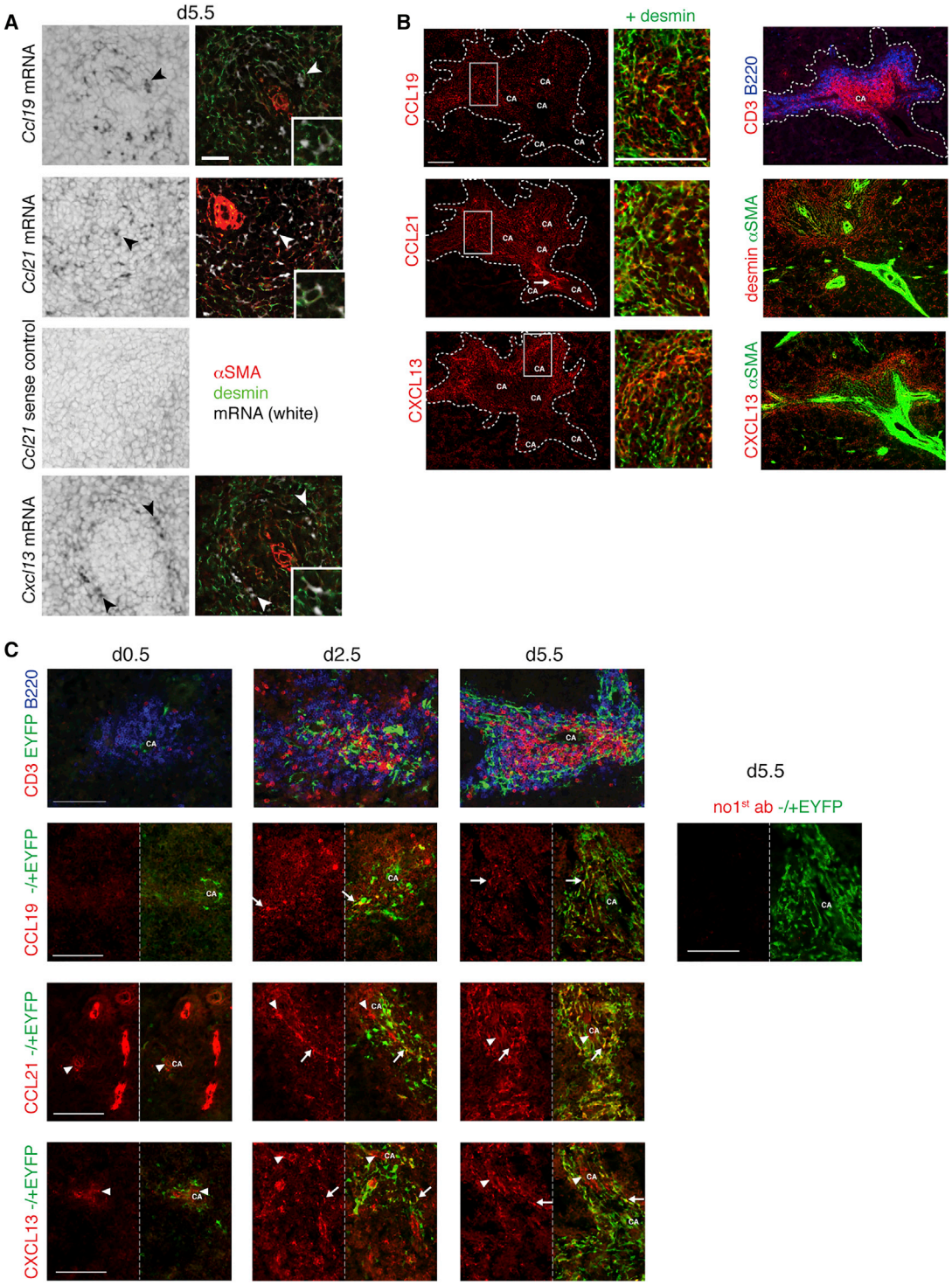

Figure 5. Desmin and αSMA Identify Two Fibroblast Cell Types within the Neonatal WP that Show Distinct Chemokine Expression Profiles

(A) *In situ* hybridization on d5.5 WT spleen with antisense probes for *Ccl19*, *Ccl21*, and *Cxcl13* as well as a sense probe as negative control for *Ccl21*. Arrowheads indicate positive *in situ* hybridization signals in black. Immunofluorescence staining for the stromal markers αSMA and desmin were performed on the same sections, with the *in situ* hybridization signal being overlaid in white (arrowheads). Insets show a close-up of a chemokine-expressing reticular cell. Scale bars represent 25 μm. (B) Immunofluorescent antibody staining on serial spleen sections of d5.5 WT mice showing compartmentalized expression of the CCL19, CCL21, and CXCL13 proteins that map with the T-B segregation. Dashed line indicates WP area on the basis of the expression of desmin$^+$ reticular cells. White rectangles indicate the area of higher resolution shown on the right with a co-staining of chemokine and desmin.

(legend continued on next page)

αSMA$^-$ B zone fibroblasts expressing CXCL13. As CCL19 expression is important for splenic T zone development, we investigated if CCL19 deficiency affects WP fibroblast development. Despite the absence of T cell clustering in d5.5 WP cords of *Ccl19*$^{-/-}$ mice, WP fibroblasts still developed into αSMA$^+$ and αSMA$^-$ desmin$^+$ cells, in ratios similar to control mice (Figure 6A). Protein staining confirmed the absence of CCL19 signals in *Ccl19*$^{-/-}$ spleen, while CCL21 and CXCL13 protein levels appeared unaltered (Figure 6B), consistent with mRNA analysis (Figure 2F). The segregation into a CCL21$^+$ and a CXCL13$^+$ zone was also maintained, but CXCL13$^+$ fibroblasts were positioned closer to the central arteriole because of the absence of T cells (Figure 6B). These data indicate that CCL19 and T cells are dispensable for the differentiation of WP fibroblasts into the two fibroblast subsets. In agreement with this conclusion, deficiency of T cells (*Tcrbd*$^{-/-}$) did not alter the development of the two fibroblast networks in d5.5 spleen (Figure 6C).

To gain deeper insight into the relative roles of B cells versus ILC3 as LTα1β2 source in WP stroma development, spleens of d5.5 *Bcr*$^{-/-}$ and *Rorc*$^{-/-}$ neonates were analyzed. WP regions of *Rorc*$^{-/-}$ mice were comparable in size with those of WT mice, with normal T and B cell zones, and the two types of WP fibroblast networks (Figures 6C and S5A). In contrast, WP cords of d5.5 *Bcr*$^{-/-}$ mice consisted of unusually compact T cell regions with an underlying desmin$^+$ fibroblast network that did not go beyond the T zone and was therefore very small (Figures 6C and S5A), resembling d0.5 WP cords of WT mice. However, most fibroblasts were αSMA$^+$ CCL21$^+$, with αSMA$^-$desmin$^+$ fibroblasts in the outer WP being reduced and hardly expressing CXCL13 (Figure 6C; not shown). Next, we investigated whether the fibroblast phenotype of d5.5 *Ltb*$^{-/-}$ mice resembles that of *Bcr*$^{-/-}$ mice. As expected (Qin et al., 2007; Vondenhoff et al., 2008; Withers et al., 2007; Zindl et al., 2009), T and B zones of d5.5 *Ltb*$^{-/-}$ spleens were very small, with a more marked reduction in T cells than B cells (Figure 6D), reminiscent of d0.5 WT spleens. The reduced T and B lymphocyte accumulation in *Ltb*$^{-/-}$ spleens was not due to diminished CCR7 and CXCR5 expression levels (Figure S6), pointing to a reduction in stromal chemokine expression as the most likely cause. *Ltb*$^{-/-}$ WP cords contained only rudimentary desmin$^+$ reticular networks around the central arteriole, with no obvious shift in the ratio of αSMA$^+$ positive fibroblasts relative to WT mice (Figures 6E and S5B). As expected, all reticular CCL19 and CCL21 protein staining was absent in d5.5 *Ltb*$^{-/-}$ WP cords. However, vessel-associated CCL21 and CXCL13 were still present (Figures 6F and S3F), thereby providing an explanation for the LT independence of these transcripts in d0–d5 spleen. In conclusion, our data show that B cells and LTα1β2 signals play a critical role in CCL19/21 expression and expansion of the desmin$^+$ fibroblast network in the developing WP.

DISCUSSION

In this study, we find that murine WP development takes place in at least four discernible stages. During stage 1 (d0.5), fibroblastic precursor cells proximal to the central arteriole are triggered to express chemokines upon encounter of LTα1β2-expressing inducer cells, mainly B cells and ILC3 (Figure S7). During stage 2 (d2.5), these desmin$^+$ and chemokine-expressing organizer cells start forming a larger network around the central arteriole while also clustering with ILC3 and an increasing number of B cells. During stage 3 (d5.5), the fibroblasts differentiate into two subsets expressing distinct chemokines that drive T cell clustering in the inner WP and B cell clustering in a ring around the T zone. During stage 4 (d8.5), T zone and B zone fibroblasts differentiate further and adopt the phenotype of adult T zone FRCs and FDCs, which coincides with clear T-B segregation and the development of polarized B cell follicles. Several lines of evidence are provided that the principal WP inducer cell is a LTα1β2-expressing B cell, while the organizer cell is a LTβR-expressing fibroblast that is triggered to express homeostatic chemokines, starting around d0.5 and continuing until adulthood. This B cell-LTo interaction drives also the expansion and differential chemokine expression by the two fibroblast subsets, eventually leading to a compartmentalized mature lymphoid tissue.

Cxcr5$^{-/-}$*Ccr7*$^{-/-}$ mice fail to develop organized splenic WP cords (Ohl et al., 2003). Here we show that CXCR5 is not critical in the early process of lymphocyte clustering in the WP, nor for the normal T and B cell accumulation, reminiscent of adult *Cxcl13*$^{-/-}$ spleens (Ansel et al., 2000). In line with these findings, we observed normal surface LTα1β2 expression on d5.5 B cells from *Cxcr5*$^{-/-}$ spleens (unpublished observations), arguing against a CXCR5-dependent feedback loop at this stage of WP development. The normal initiation of WP development in *Cxcr5*$^{-/-}$ mice is in sharp contrast to the strong defect in development of most LNs and PPs. Of note, in the few LNs developing in *Cxcl13*$^{-/-}$ mice, the early T-B accumulation and segregation occur normally, including LTα1β2 expression on *Cxcr5*$^{-/-}$ ILC3, with only the later development of FDCs and polarized follicles being defective (Cupedo et al., 2004; Luther et al., 2003). We propose that CCR7 on B cells may compensate for CXCR5 deficiency by positioning them next to the central arteriole, where we observed CCL21 expression and perivascular mesenchymal cells that may act as LTα1β2-dependent precursor cells (Sitnik et al., 2016).

In this study, we identified a limiting role for CCR7 and its ligand CCL19 in T cell accumulation and the formation of a T zone characteristic for the third stage (d5.5) of WP development, with this neonatal defect persisting into adulthood (Link et al., 2007). The B cell compartment is, however, hardly affected in neonatal and adult *Ccl19*$^{-/-}$ mice (Link et al., 2007), similar to findings in neonatal *Ccr7*$^{-/-}$ mice (Ueno et al., 2002). Contrary

(C) Immunofluorescent antibody staining of T and B cells as well as EYFP$^+$ stromal cells in spleen sections of *Rosa26-eyfp*$^{Ccl19\text{-}cre+}$ mice at indicated time points. Expression of CCL19, CCL21, and CXCL13 proteins is shown in combination with EYFP$^+$ stroma cells. Arrowheads indicate the perivascular cell layer surrounding the CA; arrows indicate the chemokine-expressing EYFP$^+$ reticulum. Data are representative of at least two independent experiments. CA, central arteriole.

Scale bars in (B) and (C) represent 100 μm.

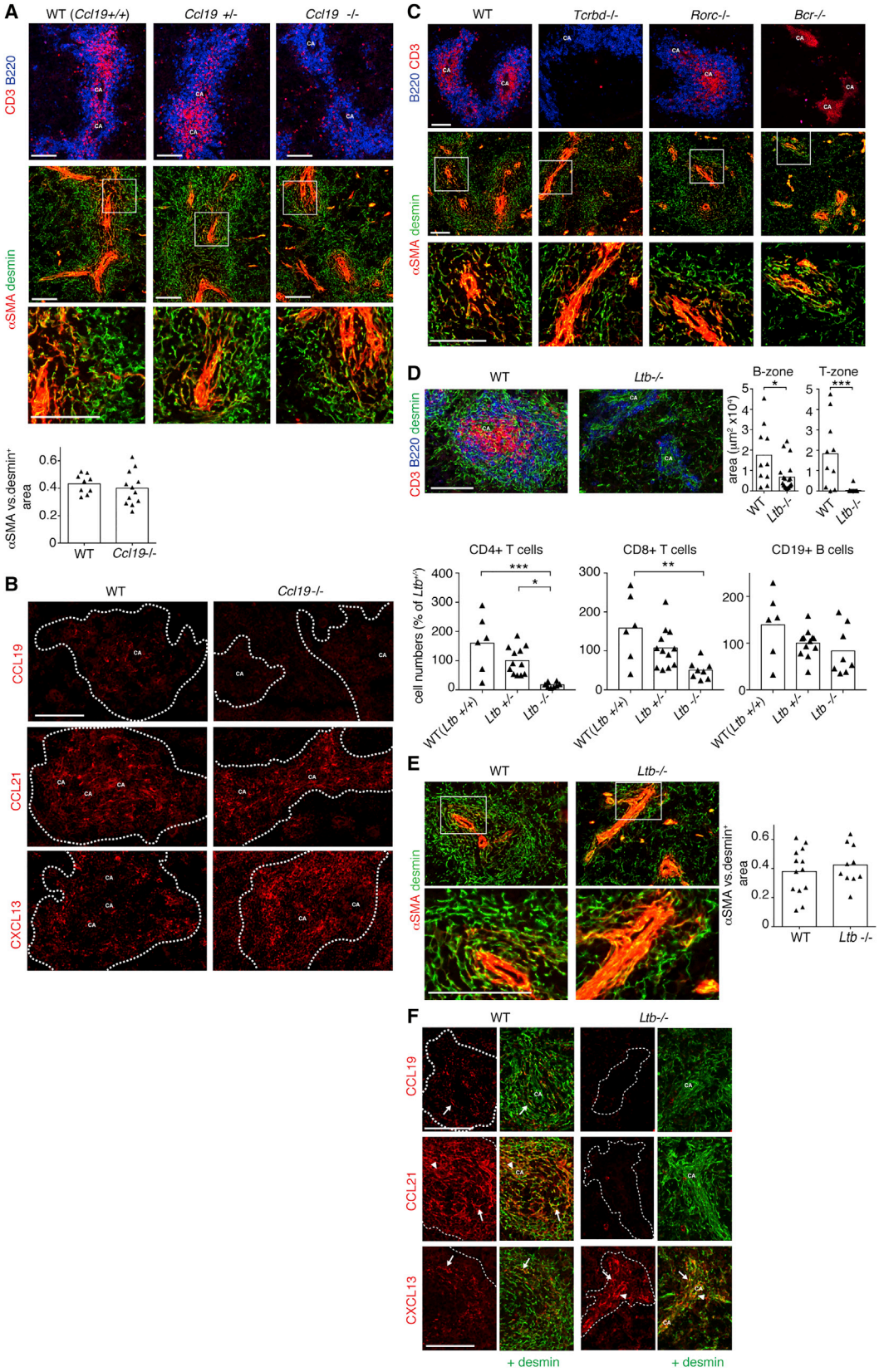

(legend on next page)

to a previous study in which neutralizing goat antibodies were used to study CCL19 function in neonates (Ueno et al., 2002), our study of *Ccl19*$^{-/-}$ neonates did not reveal a thymic defect, consistent with the normal thymic medulla of *Ccl19*$^{-/-}$ mice (Kozai et al., 2017; Link et al., 2007), leading us to propose that there is a non-redundant and thymus-independent role for CCL19 in T cell attraction and/or retention in the neonatal spleen but not LNs. This is in contrast to adult *Ccl19*$^{-/-}$ mice, in which short-term T cell homing to the spleen was found to be normal (Link et al., 2007). This neonatal spleen defect cannot be compensated for by the other CCR7 ligand, CCL21, which remains normally expressed, similar to adult *Ccl19*$^{-/-}$ SLOs (Link et al., 2007). Given that *Ccr7*$^{-/-}$ and *plt/plt* mice have a stronger splenic T cell accumulation defect than *Ccl19*$^{-/-}$ mice (data not shown) (Ueno et al., 2004), one may predict that both CCL19 and CCL21 have essential roles in forming a properly sized splenic T zone. Indeed, the recent characterization of *Ccl21*$^{-/-}$ mice shows an increased number of T cells localizing to the red pulp rather than the T zone (Kozai et al., 2017).

Here we report the quantification, localization, and regulation of early postnatal CCL19 and CCL21 when major steps in WP development occur. On d0.5, CCL21 protein was much more abundant than CCL19 and associated with neonatal lymphatic vessels, consistent with previous evidence of a vascular source in embryonic spleen (Castagnaro et al., 2013; Vondenhoff et al., 2008). We obtained no evidence for a role of these CCL21^{+} vessels in WP development, given that the early clustering of B cells and ILC3 occurred preferentially in the perivascular niche of the central arteriole and was associated with reticular desmin^{+} fibroblast networks expressing CCL21 and CCL19 protein in a LTα1β2- and B cell-dependent manner. We believe the LT dependence of fibroblastic *Ccl21* transcripts was not observed before day 5.5 because of the more abundant lymphatic CCL21 expression. On the basis of our histological evidence, we propose that CCL21 expression by mesenchymal cells may occur around the same time or shortly after CCL19 protein expression and is a consequence of the colocalization with LTα1β2-expressing B cells and ILC3.

In contrast to CCL21, CCL19 protein or mRNA expression was rarely observed in d0.5 spleen, similar to previous E18.5 data (Castagnaro et al., 2013). Fate mapping using d0.5 *Ccl19-cre* mice detected only rare fibroblastic cells next to central arteriole, but over the next 5 days, a larger *Ccl19-cre*$^{+}$ fibroblast network developed from there, covering the whole WP cord, similar to adult spleen (Chai et al., 2013; Fasnacht et al., 2014). On day 2.5, CCL19 protein colocalized exclusively with the growing reticular network of desmin^{+} *Ccl19-cre*$^{+}$ cells, thereby confirming the transgenic Cre expression pattern. Given that these cells are the only CCL19 source the time point of the early LTα1β2 signals can be mapped to d0.5–2.5, when the condensation of desmin^{+} *Ccl19-cre*$^{+}$ mesenchymal cells starts around the central arteriole and is accompanied by the co-clustering of B cells and few ILC3. It is reminiscent of embryonic clusters of ILC3 along with VCAM-1^{+} stromal cells during LN and PP development (Randall et al., 2008; Roozendaal and Mebius, 2011) and marks the start of WP growth. Consistent with this notion, mice deficient in LTβ or B cells do not proceed efficiently beyond stage 2 structures, essential for the subsequent induction of T cell attractants. In line with this finding, *Ccl19*$^{-/-}$ and *Ccr7*$^{-/-}$ spleens show a defect in the subsequent step around d5.5, when T cell accumulation usually occurs. Therefore, there seems to be a clear sequence of events with a need for clustering of LTα1β2^{+} B cells before T cells can be efficiently attracted into nascent splenic WP cords.

Both B cells and ILC3 have been proposed to act as lymphoid tissue inducer cell during WP development (Ngo et al., 2001; Tumanov et al., 2003; Vondenhoff et al., 2008; Withers et al., 2007). We observed that B cells express functional CXCR5 and CCR7 (Neely and Flajnik, 2015), similar to splenic ILC3 (data not shown) (Kim et al., 2006). B cells showed a gradual increase in LTα1β2 expression levels during the postnatal phase, with the highest levels observed in the more mature B cell subsets (Neely and Flajnik, 2015). This is in contrast to ILC3, which we found to express high LTα1β2 surface levels already before WP initiation, consistent with transcriptional data (Kim et al., 2006), but not a previous protein staining (Vondenhoff et al., 2008). The reason for this discrepancy in surface LTα1β2 staining is currently unclear. In contrast to B cells, the role of RORγ-dependent ILC3 appears not to be limiting for early WP development, as indicated by our analysis of neonatal *Rorc*$^{-/-}$, *Bcr*$^{-/-}$, *Ltb*$^{-/-}$, and *B-Ltb*$^{-/-}$ mice and consistent with adult spleen data (Cyster, 2005; Tumanov et al., 2003; Zhang et al., 2003). Therefore, we favor a model in which B cells are the critical LTα1β2-expressing inducer cell in splenic WP development (Ngo et al., 2001), with ILC3 contributing in a redundant fashion to early WP development around d0.5–2.5, when B cells are still infrequent and low in surface LT$\alpha\beta$ expression. The role of LTα1β2^{+} B cells as inducer cells and critical cytokine sources in WP development

Figure 6. The Chemokine-Expressing WP Fibroblast Network Develops Normally in the Absence of CCL19 but Not in the Absence of LTα1β2 Signals or B Cells

Immunofluorescent antibody staining for the indicated markers on spleen sections of d5.5 mice.

(A) Serial sections of *Ccl19*$^{-/-}$, *Ccl19*$^{+/-}$, and *Ccl19*$^{+/+}$ littermate control mice. WP organization is shown by T and B lymphocyte as well as stromal cell staining. White rectangles indicate the area of higher resolution depicted in the lower panel. Histological quantification of d5.5 spleen sections of WT (*Ccl19* $^{+/+}$) and *Ccl19*$^{-/-}$ mice depicts the ratio of areas positive for αSMA^{+} desmin^{+} fibroblasts relative to all desmin^{+} fibroblasts of the WP.

(B) Labeling of CCL19, CCL21, and CXCL13 proteins in WP (outlined by dashed line) of WT and *Ccl19*$^{-/-}$ mice. Dashed line indicates desmin^{+} WP area (B and F).

(C) Consecutive sections of WT, *Tcrbd*$^{-/-}$, *Rorc*$^{-/-}$, or *Bcr*$^{-/-}$ mice. Visualization of WP composition as shown in (A).

(D and E) Labeling of consecutive sections on a WT or *Ltb*$^{-/-}$ background for B and T cells (D), as well as the two fibroblast subsets (E), along with the histological quantification of the area size (D) or the ratio in areas (E) and the lymphocyte counts by flow cytometry (D).

(F) Immunofluorescence staining of chemokines in d5.5 neonates in *Ltb*$^{-/-}$ compared with WT littermates along with desmin as fibroblast marker. Arrowheads highlight the chemokine-expressing perivascular cell layer surrounding the CA; arrows indicate the chemokine-expressing desmin^{+} fibroblasts.

Data in (A)–(E) are representative of several WPs of spleens from at least two WT and knockout mice of each type. CA, central arteriole. All scale bars represent 100 μm. See also Figures S5 and S6.

is reminiscent of the previously described B cell function as LTα1β2 and TNF-α sources in FDC development and maintenance (Cyster, 2005; Tumanov et al., 2003). Of note, B cells were also observed to cluster around the central arteriole in the developing spleen of human fetuses and other vertebrates, before the arrival of T cells (Namikawa et al., 1986; Neely and Flajnik, 2016), suggesting that this is a conserved feature of WP development, possibly with B cells being also the inducer cells in humans. This raises the intriguing question of why B cells have developed this role in shaping early WP development. The spleen is evolutionary older than LNs and PPs and may have preceded ILC3 development that could have evolved simultaneously with the lymph fluid system. Therefore, ILC3 may have become essential for embryonic LN and PP anlagen formation but dispensable for the evolutionary older splenic WP development, despite their presence within developing WP cords. In support of this notion, nurse sharks have a spleen but no lymphatic system or LNs and also start WP development with B cell clustering around central arteriole (Neely and Flajnik, 2016).

The stromal LTo of the postnatal WP cord, which, upon LTβR stimulation, expresses CXCR5 and CCR7 ligands, has so far not been well defined. In embryonic spleen, Nkx2-5cre$^+$ mesenchymal cells were shown to express transcripts for *Ltbr*, *Cxcl13*, and *Vcam1*, and upon transplantation to develop into functional FRCs and FDCs organizing T and B zones, respectively (Castagnaro et al., 2013). In fetal human spleen, the organization and growth of an αSMA$^+$ reticular cell network was found to be associated with B cell accumulation and WP growth and organization (Satoh et al., 2009; Steiniger et al., 2007). Our flow cytometric analysis, cell sorting, and histological analysis of LTβR-expressing cells from neonatal spleen identified the chemokine-expressing LTo as being a mesenchymal cell type expressing not only LTβR but also PDGFRα/β, desmin, and *Ccl19-cre*. In support of its role as an organizer cell, they expressed almost all CXCR5 and CCR7 ligands inside the growing WP, formed a network, and attracted and organized the hematopoietic cells, including the inducer cells. Their growth and CCL19/21 expression appears to be strongly dependent on B cells and LTα1β2.

Our study identifies the transition from d2.5 to d5.5 as the period during which WP fibroblasts undergo a differentiation into two phenotypically and functionally distinct but physically connected desmin$^+$ fibroblast subsets, with an αSMA$^+$CCL19$^+$ reticular network in the inner WP, often coexpressing CCL21, and an αSMA$^-$ CXCL13$^+$ network in the outer WP. Interestingly, both WP fibroblast subsets have been fate mapped with *Ccl19-cre* in neonatal spleen. Therefore, either these fibroblast subsets truly originate from a common *Ccl19-cre*$^+$ mesenchymal precursor, with the outer WP fibroblasts later downregulating CCL19 expression, or they share CCL19 expression at distinct times of differentiation. Our observation that splenic WP cords in *Bcr*$^{-/-}$ and *Ltb*$^{-/-}$ mice fail to expand the desmin$^+$ reticular network of both B and T zones may support the former hypothesis of a common progenitor dependent on a growth and maturation signal. Interestingly, LTα1β2 was not required for the induction of two fibroblast subsets on the basis of αSMA expression but critical for developing CCL19/21$^+$ and CXCL13$^+$ fibroblasts and thereby T and B zone compartmentalization.

In summary, although many of the general features described for LN formation appear to be conserved during splenic WP development, including the continuous crosstalk between hematopoietic inducer and stromal organizer cells leading to a stepwise organ development, the inducer and the organizer cell types differ, as the earliest events of LN development are thought to be characterized by embryonic ILC3 interacting first with LTβR-expressing endothelial cells to initiate the vascularization of the nascent organ (Onder et al., 2017) and later on with LTβR$^+$ fibroblasts to induce the compartments before lymphocyte entry (Chai et al., 2013; Cupedo et al., 2004). In contrast, the WP is initiated perinatally within the already existing and vascularized spleen, with the development of lymphoid compartments critically depending on mature B cells interacting with LTβR$^+$ fibroblastic organizer cells. CXCR5 signals are much more critical for LN anlagen development, while CCL19/CCR7 signals have a spleen-specific role in early T zone development. Together, these findings point to distinct differences in the timing and developmental processes of the various SLOs. An improved knowledge of the steps occurring during perinatal SLO organogenesis should help in our understanding of comparable processes observed in adults. Destruction followed by reconstruction of adult WP cords has been described upon spleen transplantation (Castagnaro et al., 2013) as well as during infection with certain viruses (Castagnaro et al., 2013; Scandella et al., 2008), with disorganized lymphoid structures correlating with immunodeficiencies. Many autoimmune diseases and cancer types show the *de novo* development of local lymphoid structures, and our findings shed new light onto the roles of fibroblastic organizer cells and B cells as inducer cells in triggering and maintaining these organized lymphoid structures.

EXPERIMENTAL PROCEDURES

Mice

The following mice on a C57BL/6 background were from The Jackson Laboratory: *Ccr7*$^{-/-}$, *Cxcr5*$^{-/-}$, *Lta*$^{-/-}$, *Ltb*$^{-/-}$, *Tcrbd*$^{-/-}$, *Bcr*$^{-/-}$ (*μMT*$^{-/-}$ were used for real-time PCR and *Igh-J*$^{-/-}$ for immunofluorescence experiments), *Cd19-cre*, CD45.1$^+$, and WT C57BL/6 (B6) mice. Other mice used included *Ccl19*$^{-/-}$ (Link et al., 2007) and *Rorc*$^{-/-}$ (Sun et al., 2000). B cell-specific *Ltb*$^{-/-}$ (*B-Ltb*$^{-/-}$) mice were created by crossing *Cd19-cre* with *Ltb*$^{fl/fl}$ mice, and the deletion was tested by Southern blot analysis, as described elsewhere (Tumanov et al., 2002). CCL19 reporter mice were generated by crossing *Ccl19-cre* with *Rosa26-eyfp*$^{fl/fl}$ mice (Chai et al., 2013). All mice were maintained in pathogen-free conditions and were age and sex matched for experiments. All mouse experiments were authorized by the Swiss Federal Veterinary Office and by the University of California, San Francisco (UCSF), Institutional Animal Care and Use Committee.

Statistical Analysis

Results are reported as mean ± SD. Statistical significance for Figure 3A was determined using an unpaired two-tailed Student's t test for unequal variance. In Figure 4, Kruskal-Wallis tests were performed followed by Dunn's multiple-comparison tests to determine statistical significance. Significance is indicated as follows: *$p < 0.05$, **$p < 0.01$, and ***$p < 0.001$.

SUPPLEMENTAL INFORMATION

Supplemental Information includes Supplemental Experimental Procedures, seven figures, and one table and can be found with this article online at https://doi.org/10.1016/j.celrep.2017.10.119.

AUTHOR CONTRIBUTIONS

K.S. and M.R.B. performed most experiments and wrote the manuscript. S.F. and L.S. performed immunofluorescence histology. L.S. performed qRT-PCR. A.V.T., S.A.N., and C.F.W. provided critical material. A.V.T., E.K., T.K.A.L., and E.K. helped with flow cytometry experiments. A.L. helped with *in situ* hybridization. Data for Figures 2A, 2B, and 3 were generated by S.A.L., M.M., and Y.X. working in the lab of J.G.C. S.A.L. directed the study and wrote the manuscript. All authors contributed to the design of the study and critically reviewed the manuscript.

ACKNOWLEDGMENTS

We thank H. Acha-Orbea, J. Browning, M. Cooper, I. Ferrero, D. Finke, M. Heikenwälder, P. Launois, D. Littman, B. Ludewig, B. Marsland, T. Petrova, F. Radtke, P. Schneider, F. Tacchini-Cottier, A. Wilson, and J. Zwirner for providing reagents or mice; D. Labes for fluorescence-activated cell sorting (FACS) assistance; D. Bottinelli and J. Mold for preliminary data generation; M. Sixt and P. Anderle for discussions; and P. Aparicio Domingo for critical reading of the manuscript. This work was supported by grants from the Swiss National Science Foundation (#116896 and 130488) to S.A.L.

Received: May 5, 2017
Revised: September 8, 2017
Accepted: October 30, 2017
Published: November 28, 2017

REFERENCES

Ansel, K.M., Ngo, V.N., Hyman, P.L., Luther, S.A., Förster, R., Sedgwick, J.D., Browning, J.L., Lipp, M., and Cyster, J.G. (2000). A chemokine-driven positive feedback loop organizes lymphoid follicles. Nature *406*, 309–314.

Balogh, P., Aydar, Y., Tew, J.G., and Szakal, A.K. (2001). Ontogeny of the follicular dendritic cell phenotype and function in the postnatal murine spleen. Cell. Immunol. *214*, 45–53.

Bekiaris, V., Withers, D., Glanville, S.H., McConnell, F.M., Parnell, S.M., Kim, M.Y., Gaspal, F.M., Jenkinson, E., Sweet, C., Anderson, G., and Lane, P.J. (2007). Role of CD30 in B/T segregation in the spleen. J. Immunol. *179*, 7535–7543.

Castagnaro, L., Lenti, E., Maruzzelli, S., Spinardi, L., Migliori, E., Farinello, D., Sitia, G., Harrelson, Z., Evans, S.M., Guidotti, L.G., et al. (2013). Nkx2-5(+) islet1(+) mesenchymal precursors generate distinct spleen stromal cell subsets and participate in restoring stromal network integrity. Immunity *38*, 782–791.

Chai, Q., Onder, L., Scandella, E., Gil-Cruz, C., Perez-Shibayama, C., Cupovic, J., Danuser, R., Sparwasser, T., Luther, S.A., Thiel, V., et al. (2013). Maturation of lymph node fibroblastic reticular cells from myofibroblastic precursors is critical for antiviral immunity. Immunity *38*, 1013–1024.

Cupedo, T., Lund, F.E., Ngo, V.N., Randall, T.D., Jansen, W., Greuter, M.J., de Waal-Malefyt, R., Kraal, G., Cyster, J.G., and Mebius, R.E. (2004). Initiation of cellular organization in lymph nodes is regulated by non-B cell-derived signals and is not dependent on CXC chemokine ligand 13. J. Immunol. *173*, 4889–4896.

Cyster, J.G. (2005). Chemokines, sphingosine-1-phosphate, and cell migration in secondary lymphoid organs. Annu. Rev. Immunol. *23*, 127–159.

Fasnacht, N., Huang, H.Y., Koch, U., Favre, S., Auderset, F., Chai, Q., Onder, L., Kallert, S., Pinschewer, D.D., MacDonald, H.R., et al. (2014). Specific fibroblastic niches in secondary lymphoid organs orchestrate distinct Notch-regulated immune responses. J. Exp. Med. *211*, 2265–2279.

Förster, R., Mattis, A.E., Kremmer, E., Wolf, E., Brem, G., and Lipp, M. (1996). A putative chemokine receptor, BLR1, directs B cell migration to defined lymphoid organs and specific anatomic compartments of the spleen. Cell *87*, 1037–1047.

Förster, R., Schubel, A., Breitfeld, D., Kremmer, E., Renner-Müller, I., Wolf, E., and Lipp, M. (1999). CCR7 coordinates the primary immune response by establishing functional microenvironments in secondary lymphoid organs. Cell *99*, 23–33.

Friedberg, S.H., and Weissman, I.L. (1974). Lymphoid tissue architecture. II. Ontogeny of peripheral T and B cells in mice: evidence against Peyer's patches as the site of generation of B cells. J. Immunol. *113*, 1477–1492.

Katakai, T., Suto, H., Sugai, M., Gonda, H., Togawa, A., Suematsu, S., Ebisuno, Y., Katagiri, K., Kinashi, T., and Shimizu, A. (2008). Organizer-like reticular stromal cell layer common to adult secondary lymphoid organs. J. Immunol. *181*, 6189–6200.

Kim, M.Y., Toellner, K.M., White, A., McConnell, F.M., Gaspal, F.M., Parnell, S.M., Jenkinson, E., Anderson, G., and Lane, P.J. (2006). Neonatal and adult CD4+ CD3- cells share similar gene expression profile, and neonatal cells up-regulate OX40 ligand in response to TL1A (TNFSF15). J. Immunol. *177*, 3074–3081.

Kim, M.Y., McConnell, F.M., Gaspal, F.M., White, A., Glanville, S.H., Bekiaris, V., Walker, L.S., Caamano, J., Jenkinson, E., Anderson, G., and Lane, P.J. (2007). Function of CD4+CD3- cells in relation to B- and T-zone stroma in spleen. Blood *109*, 1602–1610.

Kozai, M., Kubo, Y., Katakai, T., Kondo, H., Kiyonari, H., Schaeuble, K., Luther, S.A., Ishimaru, N., Ohigashi, I., and Takahama, Y. (2017). Essential role of CCL21 in establishment of central self-tolerance in T cells. J. Exp. Med. *214*, 1925–1935.

Link, A., Vogt, T.K., Favre, S., Britschgi, M.R., Acha-Orbea, H., Hinz, B., Cyster, J.G., and Luther, S.A. (2007). Fibroblastic reticular cells in lymph nodes regulate the homeostasis of naive T cells. Nat. Immunol. *8*, 1255–1265.

Luther, S.A., Bidgol, A., Hargreaves, D.C., Schmidt, A., Xu, Y., Paniyadi, J., Matloubian, M., and Cyster, J.G. (2002). Differing activities of homeostatic chemokines CCL19, CCL21, and CXCL12 in lymphocyte and dendritic cell recruitment and lymphoid neogenesis. J. Immunol. *169*, 424–433.

Luther, S.A., Ansel, K.M., and Cyster, J.G. (2003). Overlapping roles of CXCL13, interleukin 7 receptor alpha, and CCR7 ligands in lymph node development. J. Exp. Med. *197*, 1191–1198.

Namikawa, R., Mizuno, T., Matsuoka, H., Fukami, H., Ueda, R., Itoh, G., Matsuyama, M., and Takahashi, T. (1986). Ontogenic development of T and B cells and non-lymphoid cells in the white pulp of human spleen. Immunology *57*, 61–69.

Neely, H.R., and Flajnik, M.F. (2015). CXCL13 responsiveness but not CXCR5 expression by late transitional B cells initiates splenic white pulp formation. J. Immunol. *194*, 2616–2623.

Neely, H.R., and Flajnik, M.F. (2016). Emergence and evolution of secondary lymphoid organs. Annu. Rev. Cell Dev. Biol. *32*, 693–711.

Ngo, V.N., Cornall, R.J., and Cyster, J.G. (2001). Splenic T zone development is B cell dependent. J. Exp. Med. *194*, 1649–1660.

Ohl, L., Bernhardt, G., Pabst, O., and Förster, R. (2003). Chemokines as organizers of primary and secondary lymphoid organs. Semin. Immunol. *15*, 249–255.

Onder, L., Morbe, U., Pikor, N., Novkovic, M., Cheng, H.W., Hehlgans, T., Pfeffer, K., Becher, B., Waisman, A., Rulicke, T., et al. (2017). Lymphatic endothelial cells control initiation of lymph node organogenesis. Immunity *47*, 80–92.e4.

Qin, J., Konno, H., Ohshima, D., Yanai, H., Motegi, H., Shimo, Y., Hirota, F., Matsumoto, M., Takaki, S., Inoue, J., and Akiyama, T. (2007). Developmental stage-dependent collaboration between the TNF receptor-associated factor 6 and lymphotoxin pathways for B cell follicle organization in secondary lymphoid organs. J. Immunol. *179*, 6799–6807.

Randall, T.D., Carragher, D.M., and Rangel-Moreno, J. (2008). Development of secondary lymphoid organs. Annu. Rev. Immunol. *26*, 627–650.

Roozendaal, R., and Mebius, R.E. (2011). Stromal cell-immune cell interactions. Annu. Rev. Immunol. *29*, 23–43.

Satoh, T., Sakurai, E., Tada, H., and Masuda, T. (2009). Ontogeny of reticular framework of white pulp and marginal zone in human spleen: immunohistochemical studies of fetal spleens from the 17th to 40th week of gestation. Cell Tissue Res. *336*, 287–297.

Scandella, E., Bolinger, B., Lattmann, E., Miller, S., Favre, S., Littman, D.R., Finke, D., Luther, S.A., Junt, T., and Ludewig, B. (2008). Restoration of lymphoid organ integrity through the interaction of lymphoid tissue-inducer cells with stroma of the T cell zone. Nat. Immunol. *9*, 667–675.

Shimizu, K., Morikawa, S., Kitahara, S., and Ezaki, T. (2009). Local lymphogenic migration pathway in normal mouse spleen. Cell Tissue Res. *338*, 423–432.

Sitnik, K.M., Wendland, K., Weishaupt, H., Uronen-Hansson, H., White, A.J., Anderson, G., Kotarsky, K., and Agace, W.W. (2016). Context-dependent development of lymphoid stroma from adult CD34(+) adventitial progenitors. Cell Rep. *14*, 2375–2388.

Steiniger, B., Ulfig, N., Risse, M., and Barth, P.J. (2007). Fetal and early postnatal development of the human spleen: from primordial arterial B cell lobules to a non-segmented organ. Histochem. Cell Biol. *128*, 205–215.

Sun, Z., Unutmaz, D., Zou, Y.R., Sunshine, M.J., Pierani, A., Brenner-Morton, S., Mebius, R.E., and Littman, D.R. (2000). Requirement for RORgamma in thymocyte survival and lymphoid organ development. Science *288*, 2369–2373.

Tumanov, A., Kuprash, D., Lagarkova, M., Grivennikov, S., Abe, K., Shakhov, A., Drutskaya, L., Stewart, C., Chervonsky, A., and Nedospasov, S. (2002). Distinct role of surface lymphotoxin expressed by B cells in the organization of secondary lymphoid tissues. Immunity *17*, 239–250.

Tumanov, A.V., Grivennikov, S.I., Shakhov, A.N., Rybtsov, S.A., Koroleva, E.P., Takeda, J., Nedospasov, S.A., and Kuprash, D.V. (2003). Dissecting the role of lymphotoxin in lymphoid organs by conditional targeting. Immunol. Rev. *195*, 106–116.

Ueno, T., Hara, K., Willis, M.S., Malin, M.A., Höpken, U.E., Gray, D.H., Matsushima, K., Lipp, M., Springer, T.A., Boyd, R.L., et al. (2002). Role for CCR7 ligands in the emigration of newly generated T lymphocytes from the neonatal thymus. Immunity *16*, 205–218.

Ueno, T., Saito, F., Gray, D.H., Kuse, S., Hieshima, K., Nakano, H., Kakiuchi, T., Lipp, M., Boyd, R.L., and Takahama, Y. (2004). CCR7 signals are essential for cortex-medulla migration of developing thymocytes. J. Exp. Med. *200*, 493–505.

Vondenhoff, M.F., Desanti, G.E., Cupedo, T., Bertrand, J.Y., Cumano, A., Kraal, G., Mebius, R.E., and Golub, R. (2008). Separation of splenic red and white pulp occurs before birth in a LTalphabeta-independent manner. J. Leukoc. Biol. *84*, 152–161.

Withers, D.R., Kim, M.Y., Bekiaris, V., Rossi, S.W., Jenkinson, W.E., Gaspal, F., McConnell, F., Caamano, J.H., Anderson, G., and Lane, P.J. (2007). The role of lymphoid tissue inducer cells in splenic white pulp development. Eur. J. Immunol. *37*, 3240–3245.

Zhang, N., Guo, J., and He, Y.W. (2003). Lymphocyte accumulation in the spleen of retinoic acid receptor-related orphan receptor gamma-deficient mice. J. Immunol. *171*, 1667–1675.

Zindl, C.L., Kim, T.H., Zeng, M., Archambault, A.S., Grayson, M.H., Choi, K., Schreiber, R.D., and Chaplin, D.D. (2009). The lymphotoxin LTalpha(1) beta(2) controls postnatal and adult spleen marginal sinus vascular structure and function. Immunity *30*, 408–420.